Applied Catalysis B: Environmental 244 (2019) 303–312

Contents lists available at ScienceDirect

Applied Catalysis B: Environmental

journal homepage: www.elsevier.com/locate/apcatb

Achieving efficient H_2O_2 production by a visible-light absorbing, highly stable photosensitized TiO_2

Tomasz Baran[a,b], Szymon Wojtyła[b], Alessandro Minguzzi[a,*], Sandra Rondinini[a,c], Alberto Vertova[a,c]

[a] Department of Chemistry, University of Milan, via Golgi 19, 20133 Milan, Italy
[b] SajTom Light Future, Węzerów 37/1, 32-090, Węzerów, Poland
[c] INSTM, Consorzio Interuniversitario per la Scienza e Tecnologia dei Materiali, Via San Giusti 9, Firenze, Italy

ARTICLE INFO

Keywords:
Photocatalysis
Surfactant degradation
Charge carrier injection
Photosensitization
Cobalt(II) 2 -ethylhexanoate

ABSTRACT

In this paper we propose titanium dioxide modified with cobalt(II) 2-ethylhexanoate (Co@TiO_2) as photoactive material for the efficient visible light driven production of H_2O_2. We demonstrate that visible light activity can be achieved thanks to a photoinduced electron transfer from the excited complex towards the TiO_2 conduction band that corresponds to a cobalt-to-titanium-charge-transfer transition. H_2O_2 is synthetized by a combination of oxygen reduction and water oxidation, that is possible thanks to the correct band position of Co@TiO_2. A mechanism of H_2O_2 formation is suggested on the basis of experimental evidences. Reactive oxygen intermediates, together with H_2O_2 are responsible for the photocatalytic degradation of a nonionic surfactant, methylene blue and phenol for wastewater treatments. Finally, and quite interestingly, Co@TiO_2 can be also used in a photoelectrochemical setup, where it can be adopted both as photoanode and photocatode, and the switching potential corresponds to the redox potential of the adsorbed complex Co(III)/Co(II) couple.

1. Introduction

The development of photocatalysts active under visible light irradiation represents one of the most important research topics in the field of photocatalysis. Due to their high band gap energy, many semiconductors, like TiO_2, CuI or ZnO, absorb mainly ultraviolet light, a small fraction of the solar radiation. A desired feature of a photocatalyst is visible light-induced activity that allow to use a significant fraction of sunlight. Several methods of photocatalysts photosensitization have been explored, including doping, surface modification by organic dyes and metal complexes, coupling with narrow band gap semiconductors (composites of two semiconductors) and deposition of metals (photosensitization due to the plasmonic effect) [1,2]. The most common methods of photosensitization by surface modification are discussed in the literature [3–6]. These methods are: direct photosensitization, photosensitization involving electron injection, involving hole injection or surface plasmon resonance. According to the first model (Fig. 1A), photosensitization can be achieved by a surface charge transfer complex formation by binding a modifier (organic or inorganic) to the semiconductor surface. The mechanism is based on a direct electron transfer through the optical excitation of a surface moiety-semiconductor complex.

A ligand-to-metal charge transfer (LMCT) or metal-to-metal charge transfer (MMCT) leads to electron injection to the conduction band. As an example for MMCT, in the case of TiO_2, the MMTC produces a reduced Ti center (Ti^{3+}), which can be considered as an electron trapped in the conduction band. Semiconductors modified with organic modifiers [7] as well as inorganic cyanide complexes [8] can be given as examples of LMCT or MMCT systems. In addition, two other two-steps mechanisms exist (Fig. 1B, C): light excitation of the surface bound chromophores, followed by a dark interfacial electron transfer from the excited state of the sensitizer to the CB of the semiconductor (photoinduced electron transfer, according to the Sakata-Hashimoto-Hiramoto model, Fig. 1 B), or a hole injection from the excited state of the sensitizer to the valence band of the semiconductor (photoinduced hole transfer, Fig. 1C) [6,9]. The recent literature reports several examples of photocatalysts or dye sensitized solar cells materials which follow these mechanisms. In particular, TiO_2 modified with platinum(IV) chloride complexes [10], chromium (III) complex [11], iron complexes with nicotinic ligand [12] or N-heterocyclic carbine ligand [13] and Ru-phthalocyanine complex [14] are examples of materials exhibiting mechanism based on electron injection. In turn, TiO_2 sensitized with chromium(VI) species [10] or Ru cluster [15] as well as copper oxide modified with the so-called N3 dye [16] can be given as examples of

* Corresponding author at: Department of Chemistry, University of Milan, via Golgi 19, 20133 Milan, Italy.
E-mail address: alessandro.minguzzi@unimi.it (A. Minguzzi).

https://doi.org/10.1016/j.apcatb.2018.11.044
Received 19 September 2018; Received in revised form 14 November 2018; Accepted 15 November 2018
Available online 17 November 2018
0926-3373/

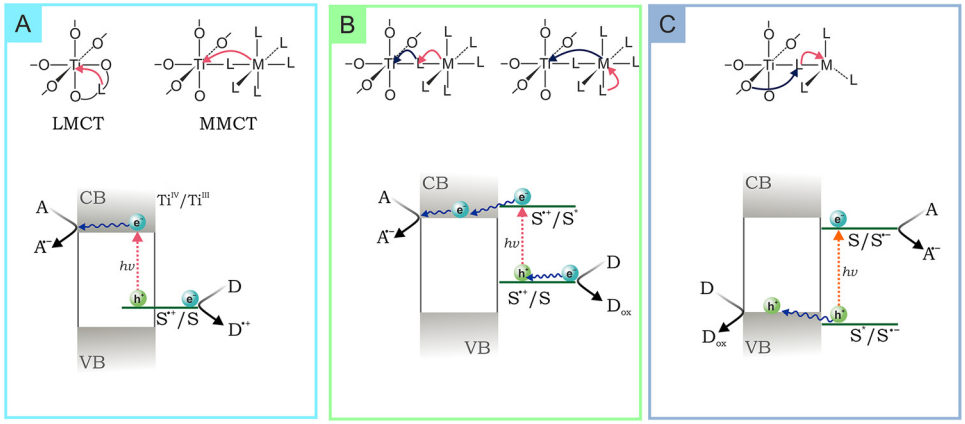

Fig. 1. Mechanisms of wide band gap semiconductors photosensitization. A - direct photosensitization (optical charge transfer), B - photosensitization involving an electron injection from the excited photosensitizer, C -photosensitization involving a hole injection to the valence band. The upper row shows a pictorial scheme of optical (red arrows) and consecutive dark (blue arrows) charges transfer processes. (Denotation: A – electron acceptor, D- electron donor, S- sensitizer, CB – conduction band, VB – valence band) (For interpretation of the references to colour in this figure legend, the reader is referred to the web version of this article).

photoinduced hole injection mechanism. An ideal sensitizer should strongly absorb visible light, have long living excited states, exists in stable oxidized and reduced forms and do not have the tendency to aggregate or degrade.

Photodriven H_2O_2 production represents a very attractive approach for the sustainable production of an advanced oxidant for purification of water and surfaces [17,18]. Many metallic and metal-free materials have been reported as photocatalysts for the synthesis of H_2O_2 [19–23]. However, their need of sacrificial electron donor such as alcohols, the poor stability under irradiation, the use of expensive, poorly abundant materials (e.g. Pt decorated TiO_2) or the low activity demonstrated in H_2O_2 synthesis request the need for better performing, visible light absorbing, low cost alternative photocatalysts.

In this paper we present a TiO_2-based material modified with cobalt (II) 2-ethylhexanoate for photocatalytic and photoelectrochemical formation of hydrogen peroxide as well as for photoinduced degradation of a detergent (Triton X-100) as a model water contaminant. Triton X-100 is a non-ionic surfactant that has a wide range of applications. In fact, non-ionic surfactants are today one of the most widely used industrial-scale class of surfactants for the production of detergents, emulsifiers, wetting agents and dispersants [24,25]. Recently, TiO_2 and other photocatalysts have been discussed as efficient materials for detergents degradation [25–28]. Czech et al. suggested a mechanism of photocatalytic degradation based on a reactive oxygen species such as hydrogen peroxide [28]. Moreover, they demonstrated that the addition of H_2O_2 influences the photo-oxidation of Triton X-100, often adopted as a model pollutant. The mechanism of photocatalytic decomposition of Triton X-100 has been proposed in the literature [25,29,30]. Four intermediates were identified: tetramethylbutylphenol, tert-octylphenoxyethanol, tertoctyl phenoxyethyl formate, and tert-octylphenoxydiethoxyl formate.

Titanium dioxide is a well-known photocatalytic material that offers a high chemical stability and photostability, has low cost, low toxicity and low environmental impact [31]. In a recent review, photocatalytic production of H_2O_2 by TiO_2 is reported as being poorly effective [32]. However, a TiO_2/graphene oxide composite has shown interesting H_2O_2 production capability by photoreduction of O_2 [33]. The stability of these systems for long operation times has not been assessed. Moreover, TiO_2 loaded with metallic alloy nanoparticles e.g. Au, Pt, Ag showed good efficiency for H_2O_2 production and several hours stability [34,35]. All listed photocatalytic materials require the presence of sacrificial electron donor such as ethanol of propanol [33–35]. An alternative way to improve the photocatalytic activity of TiO_2 is its association with other semiconductors [36].

In a previous work we demonstrated that Ni and Co titanates are promising materials for the photocatalytic and photoelectrochemical synthesis of H_2O_2 [18]. Both materials absorb visible light thanks to their favorable band gap energy (2.4 eV and 3.0 eV, respectively). Unfortunately, the stability is poor, probably due to photo-corrosion phenomena. As a possible alternative, we here propose TiO_2 modified with a cobalt complex, where photosensitization is achieved thanks to electron injection. We will demonstrate the effective, efficient and long lasting semiconductor/cobalt complex coupling and that the resulting sensitized photoactive material successfully produces hydrogen peroxide upon irradiation with visible light, particularly when used in oxygen saturated solution and in the absence of a sacrificial electron donor. The results suggest that hydrogen peroxide is generated both from oxygen reduction (by photogenerated electrons) and from water oxidation (from photogenerated holes). All these features have never been demonstrated for a single photocatalyst for H_2O_2 production in the millimolar scale. The high material's performances are also confirmed by the effective degradation of Triton X-100, methylene blue and phenol.

2. Experimental section

All commercial chemicals were used without further purification. Cobalt(II) 2-ethylhexanoate ($Co(etx)_2$) was purchased by Sigma-Aldrich.

2.1. Anatase preparation sol-gel method

3 mL of $TiCl_4$ (≥99.0%, SigmaAldrich) was added dropwise to 10 mL of ethanol (absolute grade) under continuous stirring. A light yellow solution was obtained and gelatinized for 100 h to form a gel. The latter was vaporized at 80 °C until a dry-gel was obtained, that was then calcined at 500 °C for 2 h in air to form a TiO_2 powder.

2.2. Preparation of $Co(etx)_2$@TiO_2

TiO_2 has been modified with cobalt(II) 2-ethylhexanoate (Sigma-Aldrich). A cobalt(II) 2-ethylhexanoate solutions (65%, 4 mL) was added to a TiO_2 suspensions (0.75 g dm^{-3}) in DMSO in a 1:20 modifier/TiO_2 molar ratio. The suspension was sonicated for 10 min and magnetically stirred for 12 h; afterward it was filtered, washed several times with ethanol, and dried in the air at 60 °C. This material is denoted as Co@TiO_2. All powders were stored under inert atmosphere and in the dark.

2.3. Electrode preparation

Electrodes were prepared using FTO glass (fluorine doped tin oxide - Sigma-Aldrich, surface resistivity of ~7 Ω/sq) as a substrate. FTO was previously washed with diluted H_2SO_4, water, and ethanol under ultrasounds. The material suspension was prepared in ethanol (1 mg mL^{-1}) by sonication for 5 min. Subsequently, 200 µL of the suspension were dropcasted onto clean FTO.

2.4. Characterization of materials

Diffuse reflectance spectra (DRS) in the UV–vis range were recorded using a UV-2600 spectrophotometer (*Shimadzu*) equipped with an integrating sphere (6 cm dia.). Previously dried $BaSO_4$ (puriss., Sigma-Aldrich) was used to dilute the sample in 1:50 wt. ratio (samples were ground with $BaSO_4$). $BaSO_4$ was used also as a reference material. Surface modification was studied using attenuated total reflectance-Fourier transform infrared spectroscopy (ATR-FTIR). ATR spectra were taken using an IRAffinity-1S FTIR spectrophotometer (Shimadzu) equipped with Quest ATR accessory (Specac) with extended wavelength diamond. In case of measurement with previously used photocatalyst, prior to the analysis the material was separated by centrifugation, washed 3 times with water and dried.

Structures were identified using X-ray diffraction (XRD) at X'Pert PRO (X-ray (Cu) 40 kV). EDS (Energy-Dispersive X-ray Spectroscopy) spectra were recorded using a scanning electron microscope coupled to an energy dispersive X-ray spectrometer (SEM-EDS) TM-1000 (Hitachi).

Photocurrents were measured in a 3-electrodes setup using an Autolab potentiostat (PGSTAT204). FTO covered with the material under consideration was used as the working electrode. A saturated calomel electrode (SCE) and a platinum plate were used as the reference and the counter electrode, respectively. 0.1 M K_2HPO_4 + KH_2PO_4 (pH 7) was used as supporting electrolytes. The working electrode was backside irradiated to eliminate the influence of film thickness, using a LED (λ = 350 nm, 400 nm or 565 nm purchased by Huey Jann Electronics Industry). EIS (Electrochemical Impedance Spectroscopy) experiments were performed in a three-electrode system, in which Co@TiO_2/FTO was the working electrode, Ag/AgCl and gold electrode were used as the reference electrode and the counter electrode, respectively. A BioLogic SP-150 was used as a potentiostat/frequency response analyzer. The frequencies for EIS measurement are scanned from 1 kHz to 1 mHz. Electrode was biased at −0.3 V vs reference. The solution used for EIS tests was phosphate buffer (pH 7).

2.5. Photocatalytic tests towards H_2O_2 formation

Photocatalytic tests towards H_2O_2 formation were performed in a quartz cuvette. The photocatalyst was suspended (1 g dm^{-3}) in an aqueous potassium hydrogen phthalate solution (50 mL, 0.1 M, pH = 3.9). The suspension was purged with O_2 or N_2 for 15 min before and during the experiments. The suspension was irradiated using a LED (λ = 400 nm or 565 nm).

Hydrogen peroxide was determined adopting an electrochemical method based on the use of a Au disc (1.8 mm diameter) as the working electrode [18]. The Au disc was polished with alumina powder 0.5 μm for 3 min and then sonicated in distilled water for 10 s. Cyclic voltammetry (CV, in range from 0 to 1.3 V vs SCE, scan rate 10 mV s^{-1}) were performed using an Autolab potentiostat/galvanostat (PGSTAT204) in a conventional three-electrode cell, where a saturated calomel electrode (SCE) and a platinum plate were used as the reference and the counter electrode, respectively. H_2O_2 concentration, C_{H2O2} was determined through a calibration straight line, described by the following equation:

$$C_{H2O2} = \frac{I_p + 6.024 \cdot 10^{-7}}{0.0274}$$

where I_p is the current of the anodic peak at about 1.1 V vs SCE. The calibration curve was obtained using solutions containing known amounts of hydrogen peroxide in the concentration range 0.001–10 mM.

2.6. Photocatalytic degradation of Triton X-100

5 mg of photocatalyst were added to 50 mL of a 50 mg L^{-1} Triton X-100 aqueous solution. The solution was sonicated for 5 min, left in dark for 30 min and then irradiated under LED 400 nm illumination for 90 min. The solution was sampled every 15 min, filtered using syringe filters (RC 0.22 μm) and analyzed using an UV-2600 spectrophotometer (*Shimadzu*). Similar tests were performed with other model pollutants: 25μM aqueous thiazine dye - methylene blue (*Chempur*) and 0.5 mM aqueous phenol (*Chempur*).

2.7. Hydroxyl radical quenching

The determination of the amount of produced $OH^{\cdot}$ was carried out using the terephthalic acid fluorescence probe method. An aqueous solution (3.5 mL) containing 0.01 M NaOH, 0.5 mM terephthalic acid and 3 mg of Co@TiO_2 was prepared and sonicated for 10 min in the dark. Subsequently, the suspension was transferred to quartz fluorescence cuvette and irradiated for 10 min using LED 400 nm light source. Fluorescence spectra of the suspension were measured with a fluorescence spectrophotometer (FluoroLog-3, Horiba, *Jobin-Yvon*). Excitation wavelength was 315 nm.

2.8. Superoxide anion radical detection

A thin film of the photocatalyst was prepared on an ITO foil (Indium tin oxide coated PET, *Sigma Aldrich*) from dichloromethane suspension (1 mg ml^{-1}). The film was placed (on a sidewall to not disrupt the absorption measurements) in the quartz fluorescence cuvette (1 cm × 1 cm) filled with 0.1 M tetrabutylammonium perchlorate solution in acetonitrile (extra dry) under N_2 or O_2 atmosphere. Thin film was irradiated for 1, 2 and 3 min. UV–vis absorption spectra were collected immediately after irradiation using UV-2600 spectrophotometer (*Shimadzu*).

3. Results

Titanium dioxide (TiO_2), being prepared by calcination at 500 °C, is composed by the anatase structure, as demonstrated by XRD diffractograms shown in Fig. 2A (anatase - space group: I 41/a m d (141)), where peaks at 2θ = 25, 37, 48, 53, 54, 62, 69 and 71° were assigned to the 101, 004, 200, 105, 211, 204, 116, 215, diffraction peaks of anatase TiO_2 (JCPDS No. 21–1272) [37]. Modification of anatase with the Co-complex was performed by impregnation. The presence of cobalt(II) 2-ethylhexanoate complex does not affect the structure of titanium dioxide as demonstrated by XRD (Fig. 2A).

In addition, ART-IR proved the success of semiconductor's surface modification. The ATR spectrum of neat TiO_2 shows a ν(OH) stretching band between 3700 and 3300 cm^{-1}, as shown in Fig. 2B. The broad band can be attributed to hydroxyl groups at TiO_2 surface [38]. High absorbance below 1000 cm^{-1} origins form Ti-O-Ti bonds vibrations [39]. The spectrum of titanium dioxide modified by cobalt(II) complex showed a few additional bands, e.g. in the region between 3020 and 2740 cm^{-1} and in the region between 1690 and 1200 cm^{-1}. These correspond to the main band of cobalt(II) 2-ethylhexanoate. Since Co@TiO_2 was washed several times with ethanol to remove the unbound complex, FTIR spectra prove the adsorption of the cobalt complex at the TiO_2 surface.

The presence of surface modifiers is confirmed also by Energy-Dispersive X-ray Spectroscopy (EDX). Characteristic peaks of Co (Kα 6.93 keV and Kβ 7.65 keV) were observed, as shown in Fig. 2C. Moreover, the EDX mapping (Fig. 2D) indicated a fairly uniform elemental distribution of titanium, oxygen and cobalt over the particles, confirming that the cobalt complex was well dispersed on the semiconductor.

Surface modification is expected to affect the electronic properties of a photocatalyst. As described above, the goal of this research is to make the semiconductor active in the visible-light range, possibly using direct irradiation with solar light. Diffuse reflectance spectra, transformed to Kubelka–Munk function, together with the absorption spectrum of the metal complex are shown in Fig. 3. The cobalt(II) 2-

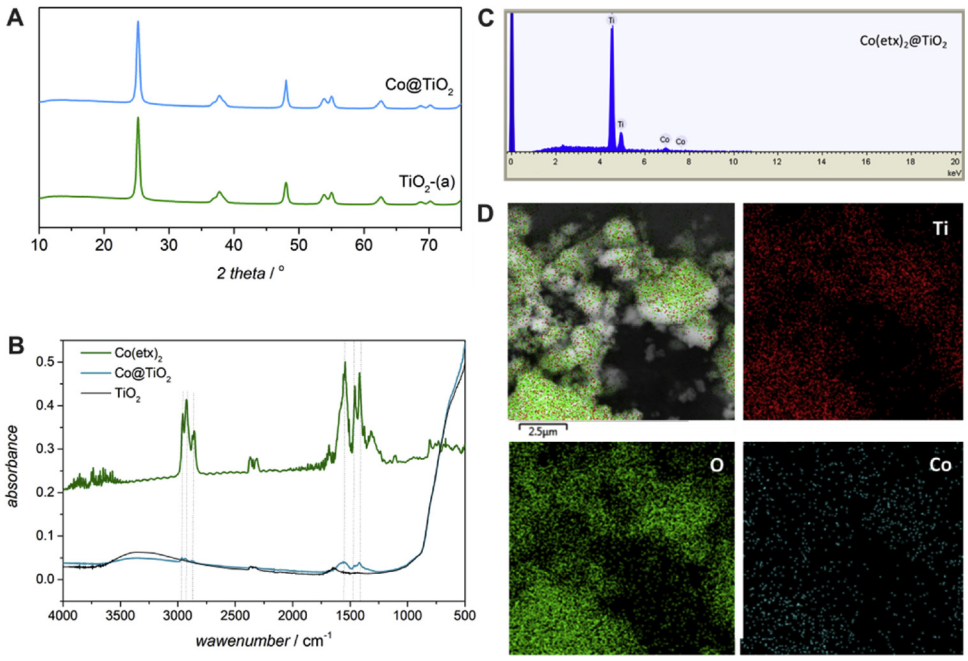

Fig. 2. Physico-chemical characterizations. A - XRD diffractograms for anatase (green curve) and Co@TiO2 (light blue curve). B – ATR-FTIR spectra of neat and modified titanium dioxide as well as spectrum of cobalt(II) 2-ethylhexanoate. C – EDX spectrum of Co@TiO_2. D – SEM-EDX image of Co@TiO_2 overlayed with the composite elemental map (titanium, oxygen and cobalt). (For interpretation of the references to colour in this figure legend, the reader is referred to the web version of this article).

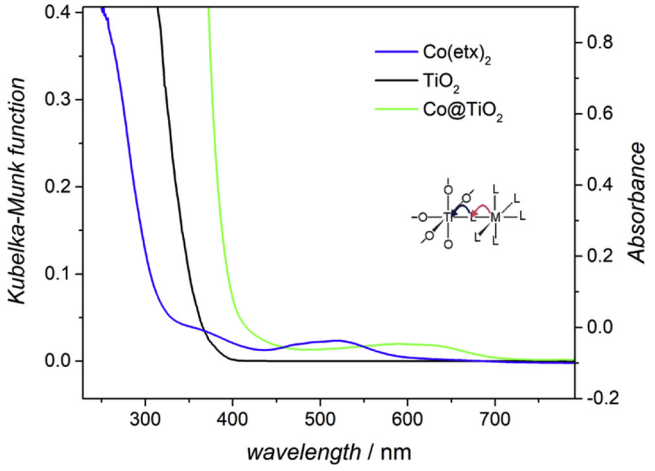

Fig. 3. Diffuse reflectance spectra of neat and modified TiO_2 (left axis) and UV–vis spectrum of cobalt complex (right axis). (For interpretation of the references to colour in this figure legend, the reader is referred to the web version of this article).

ethylhexanoate spectrum, with a charge-transfer band at about 500 nm, is typical of octahedral cobalt complexes [40]. In contrast to bare TiO_2, Co@TiO_2 absorbs visible light, which is in turn a consequence of spectral properties of the adsorbed photosensitizers. Light induced metal-to-metal charge transfer (Fig. 3, inset) results into a bathochromic shift of the absorption onset (about 70 nm in comparison with neat TiO_2), similarly to what observed for TiO_2 doped with Co ions [41]. In the case of a similar material, based on a different metal but with the same ligand (TiO_2 / nickel(II) 2-ethylhexanoate) the bathochromic shift was not observed (see fig. S1 in Supporting Information).

In addition, the spectrum of Co@TiO_2 shows a weak LMCT (ligand to cobalt) band centred at about 600 nm, shifted in comparison with the free complex (when the band lays at about 500 nm, blue curve in Fig. 3) thanks to interactions with TiO_2. The material's band gap energy has been determined according to the Tauc theory [42] considering an indirect semiconductors, as TiO_2 is, since surface modifications is not supposed to have any influence in this sense. The determined band gap of Co@TiO_2 is 2.95 eV, which differs significantly from that of neat titanium dioxide (3.2 eV), thus demonstrating a significant influence of this surface modification on the electronic structure of TiO_2. It should be highlighted that a simple mixture of TiO_2 and cobalt complex shows a different spectrum than Co@TiO_2.

The redox properties of cobalt(II) 2-ethylhexanoate complexes were studied using cyclic voltammetry, as it is described in the Supporting Information (figure S2). The determined redox potential of the cobalt complex is 0.79 V vs the reversible hydrogen electrode (RHE).

Considering an illuminated semiconductor immersed into an electrolyte and connected to a counter electrode, the photocurrent density is directly related to the efficiency of charge carriers (electrons and holes) generation and transfer. Not-modified titanium dioxide generates anodic photocurrents within a wide potentials window, upon UV illumination. However, its inactivity in visible light is well known [12,43]. On the contrary, Co@TiO_2 generates photocurrents upon ultraviolet (λ = 350 nm - Fig. 4 A) as well as under visible light (λ = 565 nm - Fig. 4 B). Moreover, a photocurrent switching effect is evident: either anodic or cathodic photocurrents are generated, depending on the applied potential. This phenomenon, sometimes referred to as anomalous photoeffect (APE) have been previously observed as a crossover of dark and light current/potential characteristics [44]. The origin of APE is still not understood, but is likely bound to either the presence of surface state, that can induce a partial Fermi level pinning (band unpinning) and that are found to accumulate charge around the switch potential [45], or to the presence of an adsorbed redox couple, inducing the so-called PEPS (photoelectrochemical photocurrent switching) effect, which implies also a photocurrent shift in dependence on the incident wavelength [46]. In the present case the photocurrent sign switch appears to be independent on the incident light wavelength, still the photocurrent density under UV is significantly higher than under visible light. Note that the photocurrent switching effect was not observed in the case of a control material, i.e. titanium dioxide modified with sodium tris-carbonatocobaltate(III) (synthesis and photoelectrochemical characterization are described in the Supporting Information, fig. S3). This likely means that the photocurrent switching phenomenon is directly related to the presence of the cobalt(II) complex, while the adoption of a cobalt(III) complex is not effective.

In addition, photocurrents in oxygen atmosphere are just slightly higher than in N_2-saturated electrolyte. It is interesting to observe the role of dissolved O_2: as expected, photocathodic currents significantly

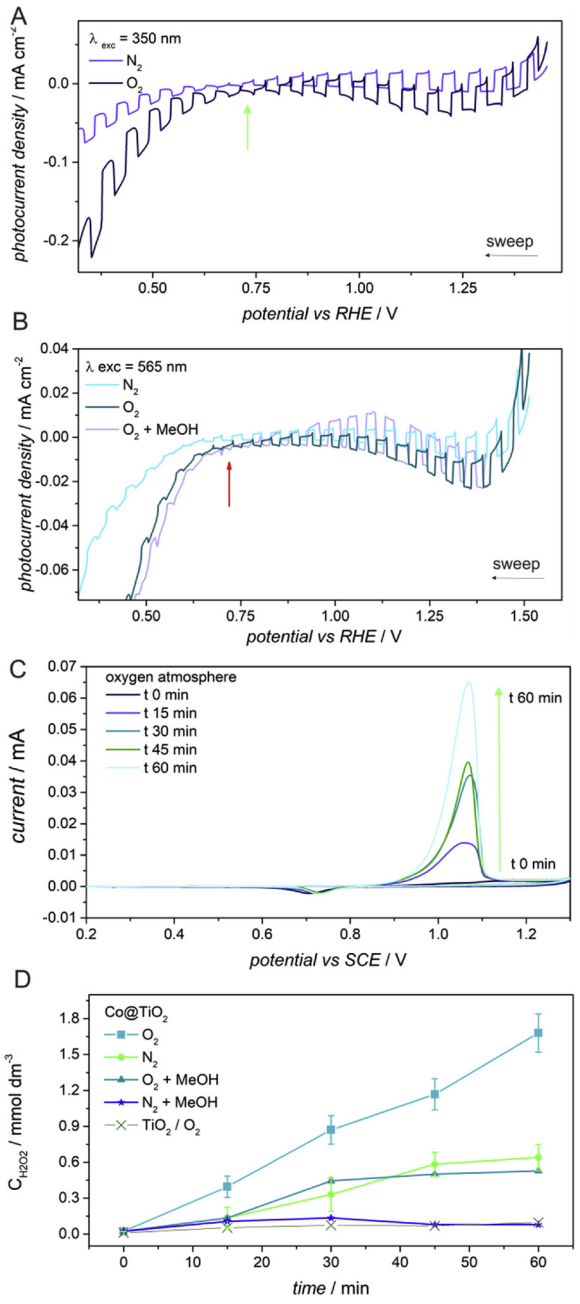

Fig. 4. Photoactivity of Co@TiO_2. Photocurrent analysis upon ultraviolet (A) and visible light (B) irradiation. Cyclic voltammetries on Au for determining H_2O_2 concentration (C). Results of photocatalytic tests as H_2O_2 formation upon irradiation with light λ = 400 nm in electrolyte (0.1 M potassium hydrogen phthalate solution) of pH 3.9 bubbled with O_2 or N_2 or with addition of methanol in O_2 or N_2 atmosphere (D). The concentration of the powder dispersion was set to 1 g L^{-1}. Error bars added to the one curve is based on a standard deviation from 3 independent experiments.

increase in its presence, whereas photoanodic ones are much less affected. Interestingly, the presence of methanol (MeOH) under 565 nm illumination does not significantly improve the anodic photocurrent, meaning that the latter has to be mainly assigned to water oxidation.

Co@TiO_2 was tested as a photocatalyst towards the formation of hydrogen peroxide in the presence and absence of both oxygen and methanol. H_2O_2 was detected in the irradiated photocatalyst suspension, using cyclic voltammetry with a gold working electrode, as shown in Fig. 4 C. The wavelength (400 nm) was chosen in order to be sufficient to excite Co@TiO_2 but not a bare anatase powder (see Fig. 3). The highest rate of H_2O_2 formation was observed in oxygen saturated suspension (Fig. 4 D), whereas in its absence (nitrogen saturated solution) H_2O_2 was also formed but with noticeable lower rate. Methanol was added as a sacrificial hole scavenger, and in this case hydrogen peroxide was produced only in the presence of oxygen – methanol oxidation by positive charges is in competition with water oxidation and therefore addition of methanol decreases the rate of H_2O_2 formation. Therefore, in the presence of methanol, H_2O_2 comes from O_2 activation only. All results in turn suggest that hydrogen peroxide is formed both after O_2 reduction by conduction band electrons and because of water oxidation by valence band holes (by the HOMO of the oxidized Co complex). In fact, C_{H2O2} doubles after 60 min in the case of the O_2 saturated solution with respect to the N_2 saturated solution and in the presence of both O_2 and MeOH. A control test was performed using unsensitized TiO_2, that resulted to be inactive (Fig. 4 D). Another control experiment proved that irradiating an aqueous solution of cobalt(II) 2-ethylhexanoate solution does not lead to H_2O_2 formation (figure S4).

The high activity demonstrated by Co@TiO_2 on H_2O_2 synthesis prompted us to further investigate the reaction mechanism, in turn identifying the intermediate involved.

$HO^{\bullet}$ radicals were detected by quenching with terephtalic acid. The formation of hydroxyl radicals and superoxide anion radicals has been investigated to clarify the mechanism of photocatalytic H_2O_2 production. Terephtalic acid is a well-known hydroxyl radical scavenger, which does not react with other reactive oxygen species such as $O_2^{\bullet-}$ or H_2O_2 and can therefore be used as selective sensor for $HO^{\bullet}$ [47]. The oxidation of terephtalic acid by $HO^{\bullet}$ leads to 2-hydroxyterephthalic acid, that can be easily detected by fluorescence measurement (λ_{exc} = 315 nm, λ_{emm} = 425 nm). Irradiation of a Co@TiO_2 suspension in the presence of terephtalic acid resulted in increasing emission at 425 nm, as shown in Fig. 5A. This is clear evidence of $HO^{\bullet}$ formation upon irradiation. In turn, formation of superoxide anion radical in water saturated with oxygen has been confirmed by the photo-spectroscopic approach, described elsewhere [48]. Irradiation of Co@TiO_2 thin film placed in 0.1 M solution of tetrabutylammonium perchlorate (in acetonitrile) saturated with oxygen leads to the increase of new absorption band at λ_{max} = 253 nm (see Fig. 5B), that can be associated to the formation of superoxide anion radicals [48]. These changes were not observed when the oxygen was removed from the solution by nitrogen bubbling.

Thanks to the selectivity demonstrated towards $O_2^{\bullet-}$ and $HO^{\bullet}$ formation, it is highly expected to observe a high activity with respect to the oxidation of model organic pollutants.

Co@TiO_2 was thus tested in view of its possible use in water treatment using Triton X-100 as a model pollutant [28]. Co@TiO_2 showed photocatalytic activity towards Triton X-100 degradation, as shown in Fig. 6. The surfactant concentration was determined by UV–vis spectroscopy (decrease of the 223 nm band), as discussed elsewhere [30]. The degradation experiment was initially (for 30 min) performed in the dark to obtain dark absorption-desorption equilibrium and to demonstrate the role of light. The decrease of Triton X-100 concentration in the dark was noticeable but it did not exceed 5% (that is likely compatible with the experimental error of Triton concentration), whereas a significant improvement in degradation efficiencies was observed when the light was turned on. Once again, this evidence the role of both photogenerated holes and electrons: the comparison of efficiencies in the presence and absence of oxygen points that typical oxidation by $OH^{\bullet}$ is not the sole pathway of Triton degradation, but is accompanied by O_2 reduction products. Under N_2 atmosphere Triton X-100 can be degraded because $OH^{\bullet}$ radicals from oxidation of water are formed. In addition, the ongoing degradation after 2 h demonstrate the superior stability of the here proposed photocatalyst. The degradation in the presence of unmodified titanium dioxide is negligible, a very moderate decrease of Triton X-100 concentration is observed, most likely due to its adsorption on the photocatalyst surface. A similar effect is visible in all other conditions in the dark, where under O_2 and in air

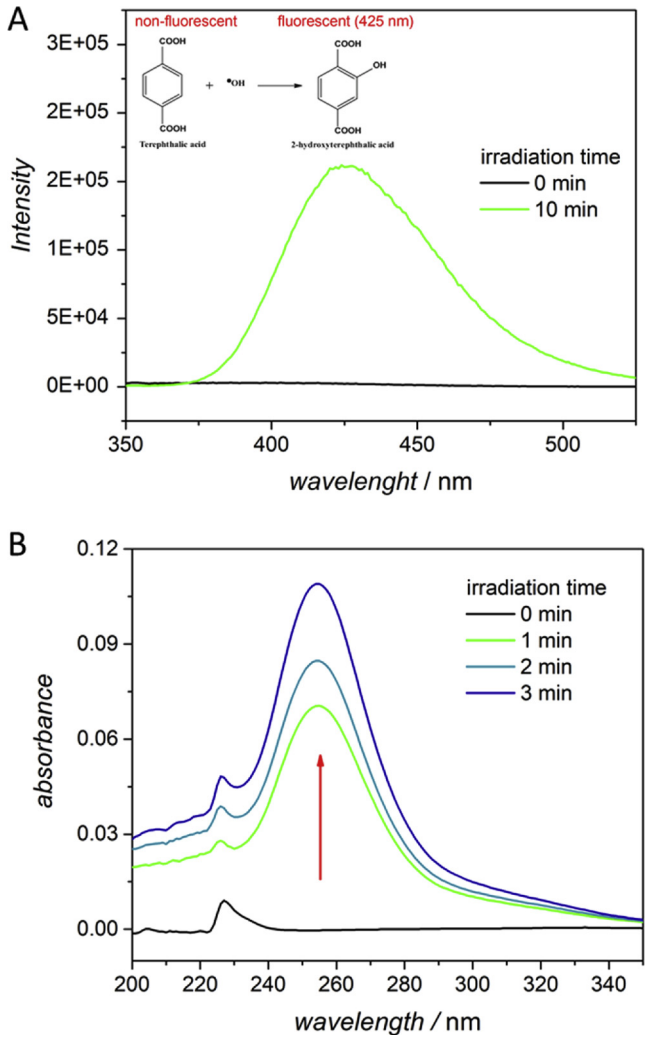

Fig. 5. Detection of H_2O_2 intermediates. A – fluorescence terephthalic acid probe for hydroxyl radicals, B- detection of superoxide anion radical.

(blue and dark green curves, respectively), there's a more pronounced decrease of absorbance than under N_2 bubbling. We believe that this is simply due to the error associated with the experimental determination of the concentration (see the error bars in Fig. 6). Indeed, a prolonged test in the dark and under O_2 bubbling, shown in the SI (figure S5), reports a smaller decrease.

In order to prove that the here proposed photocatalytic decontamination is effective also with other model pollutants, we report the results obtained adopting phenol and methylene blue. Both compounds are often used for evaluating the photocatalytic activity and their degradation mechanisms have been earlier proposed [49,50].The results of photocatalytic degradations of methylene blue and phenol are reported in Fig. 7. The degradation of methylene blue is witnessed by the decrease of peaks at 290 and 650 nm. The solution bleaching is evident from the inset picture. A 1-hour irradiation in the presence of Co@TiO_2 resulted in the degradation of approximately 60% of initial methylene blue, while neat titanium dioxide showed a significantly lower activity.

The decomposition of phenol was followed by the decrease of the 265 nm peak and 30% of phenol was removed after illumination for 90 min.

Material's stability was investigated by means of long time photocurrent generation, spectroscopic comparison between a fresh and a "used" photocatalyst as well as by EIS measurements. As shown in Fig. 8A Co@TiO_2 deposited on a conductive support can generate photocurrent under chopped light for at least 7 h without significant decrease of activity. Fig. 8B shows an FTIR spectrum of freshly prepared Co@TiO_2 and material used previously in 2 h photocatalytic H_2O_2 formation. No significant changes of spectrum have been found – spectrum of used material still showed bands assigned to the cobalt complex.

The EIS measurement was performed in the frequency range from 1 kHz to 1 mHz. Fig. 8C shows the Nyquist plots of new and used (in experiment shown in Fig. 8A) Co@TiO_2 electrodes in the dark. The impedance spectra were fitted by the equivalent circuit containing in series connected resistance with the parallel connected resistance and capacitance (see Fig. 8C-inset). A larger curvature radius usually represents a larger charge transfer resistance and a lower separation efficiency of the photogenerated electron-hole pairs [51,52]. The circular radius of new Co@TiO_2 is smaller than that of previously used material indicating that during irradiation some processes had occurred that resulted in the rise of the electron-hole recombination rate.

4. Discussion

In this paper, we demonstrated the effective photosensitization of titanium dioxide with a cobalt(II) complex, which is functional for the

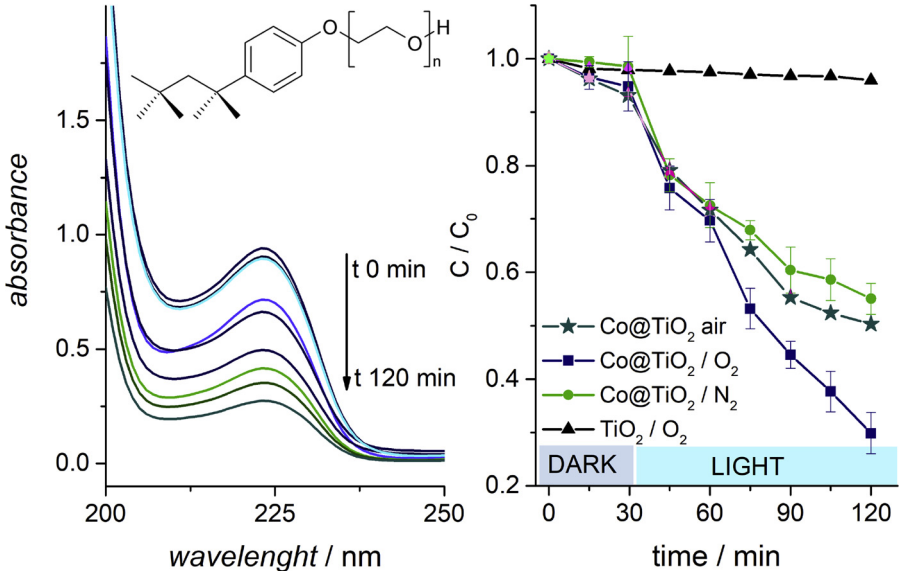

Fig. 6. Photocatalytic degradation of Triton X-100 using a 400 nm LED as source of illumination. On the left – changes of UV–vis spectra upon irradiation in the presence of Co@TiO_2 (50 mg L^{-1}). Efficiency of photocatalytic degradation of Triton X-100 in the presence of Co@TiO_2 in oxygen and nitrogen saturated solution (blue squares and green circles, respectively) and in still, not degassed (dark green stars) distilled water. Error bars are based on double repetition tests. Control test – unmodified TiO_2 (black triangles) (For interpretation of the references to colour in this figure legend, the reader is referred to the web version of this article).

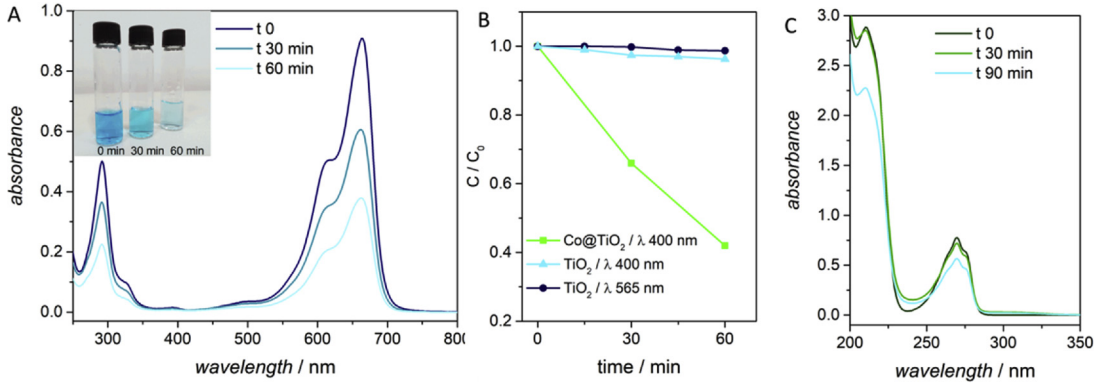

Fig. 7. Photocatalytic degradation of methylene blue and phenol as model pollutants. A - UV–vis spectra of methylene blue aqueous solution at different times during its photocatalytic degradation ($Co@TiO_2$ λ 400 nm). B - kinetic curves of photocatalytic degradation of methylene blue on $Co@TiO_2$, control tests were performed using unmodified TiO_2 using different wavelengths, as indicated in the legend. C- UV–vis spectra of phenol solution at different times during the photocatalytic degradation (For interpretation of the references to colour in this figure legend, the reader is referred to the web version of this article).

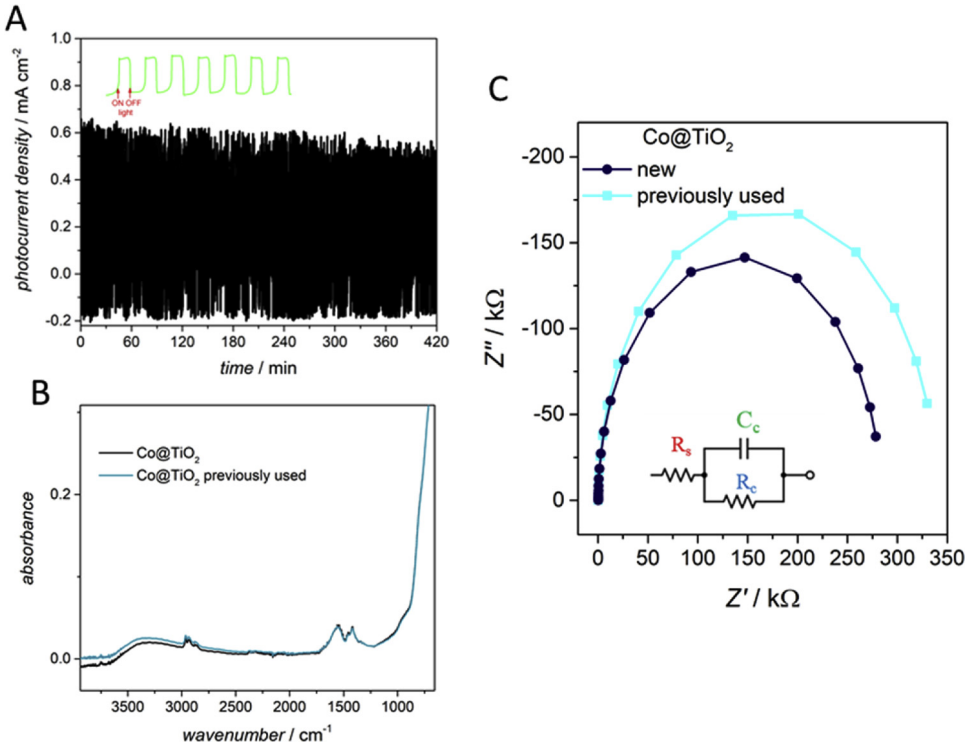

Fig. 8. Investigation of $Co@TiO_2$ stability. A – chronoamperometric measurement at 1 V vs. RHE, in phosphate buffer (pH 7) under chopped light irradiation (dark time 16 s, light time 12 s). Inset – a zoomed first 3 min of curve. B – FTIR ATR spectra of freshly prepared $Co@TiO_2$ and material used previously in 2 h photocatalytic experiment. C – Nyquist plot of $Co@TiO_2$ deposited on FTO and electrodes after 7 h irradiation under chopped light (from experiment shown in Fig. 6A).

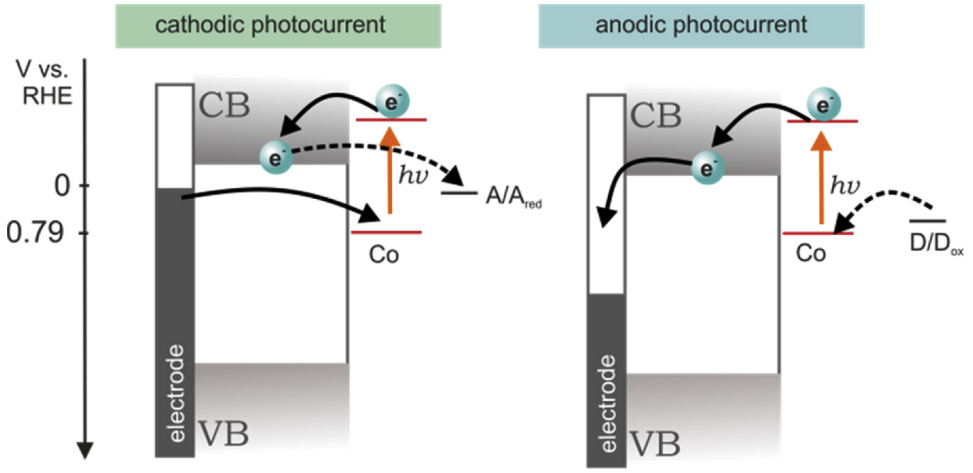

Fig. 9. The proposed mechanism of photocurrent generation on titanium dioxide modified with cobalt(II) complex. Left - cathodic photocurrents generated upon more negative potentials and right - anodic photocurrents generated at more positive potentials. Grey vertical bar indicates the electrode (e.g. metal or FTO) potential. The marked potential (0.79 V) represents the redox potential of the cobalt complex (For interpretation of the references to colour in this figure legend, the reader is referred to the web version of this article).

Table 1
Concentration of H_2O_2 after 60 min of irradiation in various conditions.

	O_2	O_2 + MeOH	N_2
Co@TiO_2 (1 g dm^{-3})	1.71 mmol dm^{-3}	0.53 mmol dm^{-3}	0.65 mmol dm^{-3}

production of H_2O_2 and in the wastewater treatment of TritonX-100, as proven by photocatalytic and photoelectrochemical experiments. Diffuse reflectance spectroscopy showed that Co@TiO_2 has a noticeable broader light absorption range than bare anatase-TiO_2. In fact: i) the band gap is reduced of about 0.25 eV thanks to metal-to-metal charge transfer (cobalt→titanium), ii) an additional charge transfer band (from the adsorbed complex) was observed in the visible light range at ~600 nm.

We can conclude that Co@TiO_2 allows visible light activity thanks to a photoinduced electron injection from the excited complex to the TiO_2 conduction band, as an effect of a MMCT transition (see Fig. 1B). As expected, illumination of pure titanium dioxide with ultraviolet light leads to anodic photocurrent [12,53]. On the other hand, here we observed the generation of both anodic and cathodic photocurrents at wavelength that excite either the semiconductor or the dye. In the first case, the mechanism could be related to what was recently proposed in the case of $BiVO_4$ [45]: the partial band unpinning (in turn due to Fermi level pinning caused by surface states) allows the possible shift of band edge energies, that is not possible in the case of band pinning, and that is at the basis of the possibility of both electrons and hole transfers. On the other hand, under visible light, the effect can be explained by the mechanism schematically shown in Fig. 9: at $E < 0.79$ V, light absorption by the reduced complex results in the excitation of the surface species with concomitant formation of unoccupied energy levels within the band gap of titanium dioxide. Electrons from the excited complex are injected into conduction band of titanium dioxide and can further promote the reduction of an electron acceptor (A) such as oxygen; at more positive potentials (right part of Fig. 10), the irradiation results in anodic photocurrents due to electron transfer from the excited complex to the conduction band of TiO_2 and further towards the conducting support (FTO). This mechanism represents an example of photosensitization based on electron injection mechanism [3]. These proposed mechanisms well explain the here collected results, which are summarized in Table 1.

For what concerns the photocatalytic activity of Co@TiO_2, the concentration of H_2O_2 obtained under different experimental conditions (Fig. 4) are summarized in Table1.

Different routes for photocatalytic or photoelectrochemical formation of H_2O_2 can be considered [18]. First of all, as illustrated in reactions 1 − 4, it can be formed via reduction of oxygen by photogenerated electrons.

$$O_2 + e_{CB}^- \rightarrow O_2^{\bullet -} \ (-0.33\ V\ vs\ NHE) \quad (1)$$

$$O_2^{\bullet -} + H^+ \rightarrow HO_2^{\bullet} \quad (2)$$

$$HO_2^{\bullet} + HO_2^{\bullet} \rightarrow H_2O_2 + O_2 \quad (3)$$

$$2O_2^{\bullet -} + 2H_2O \rightarrow H_2O_2 + O_2 + 2OH^- \quad (4)$$

Obviously, formation of H_2O_2 via two-electrons oxygen reduction could also considered:

$$O_2 + 2H^+ + 2e^- \rightarrow H_2O_2\ (0.68\ V\ vs\ NHE) \quad (5)$$

The second possible pathway is based on water oxidation to hydroxyl radical by a photogenerated hole followed by radical recombination (eq. 6–7).

$$H_2O + h_{VB}^+ \rightarrow OH^{\bullet} + H^+ (2.7V\ vs\ NHE) \quad (6)$$

$$OH^{\bullet} + OH^{\bullet} \rightarrow H_2O_2 \quad (7)$$

Indeed, we have proven the formation of $O_2^{\bullet -}$ and $OH^{\bullet}$ by spectroscopic methods.

It has been demonstrated in the literature that photocatalysts are able to remove organic and inorganic pollutants as well as microorganisms by direct reduction and/or oxidation processes (electron or hole induced reactions) or through generated reactive oxygen species (ROS) such as hydrogen peroxide, hydroxyl radical, singlet oxygen [47,54,55]. H_2O_2 is known as a powerful oxidizing agent to reach complete mineralization (process leading to H_2O and CO_2). Moreover, ROS are easily deactivated thus making the method useful for drinking water treatment and industrial water purification. Using Triton X-100, methylene blue and phenol as model pollutant, we here showed the effectiveness of the material towards wastewater treatment.

Different pathways have been proposed for the decomposition of Triton X-100. For example, Pardo et al. described an oxidation sequence induced by an hydroxyl radical attacking the polyethoxylated chain from two sides [29]. In the case of a photocatalytic process, different reactive oxygen species can react with Triton X-100 simultaneously, resulting in its mineralization. We proved that also H_2O_2 may also decompose the Triton molecule (see fig. S6) [56], but we can exclude that it is the sole responsible. In fact, H_2O_2 absorbs UV light in the same range as Triton, thus we would have noticed its presence during photocatalytic oxidation experiments (Fig. 6). This means that Triton is most likely oxidized by a combined action by photogenerated radicals and H_2O_2.

5. Conclusions

Titanium dioxide has been modified by cobalt(II) complexes to obtain photo(electro)catalysts active under visible light. Surface modification by cobalt(II) 2-ethylhexanoate has been evidenced by spectroscopic analysis, electrochemical characterization as well as photoelectrochemical tests towards hydrogen peroxide formation. We found that Co@TiO_2 successfully produces a high concentration of H_2O_2, in particular in oxygen saturated solutions. The collected results suggest that hydrogen peroxide is produced both from oxygen reduction (by photogenerated electrons) and from water oxidation (from photogenerated holes), in the absence of additional sacrificial electron donors.

The material was also investigated as photocatalyst for water treatment, using Triton X-100, methylene blue and phenol as model pollutants: its degradation was significantly higher in the presence of oxygen than in a nitrogen saturated suspension thus suggesting that, using Co@TiO_2, pollutants can be degraded by a combined production of reactive oxygen species namely $^{\bullet}OH$, $O_2^{\bullet -}$ and H_2O_2.

Acknowledgements

We thank Dr. Claudio Carrara and Dr. Emanuele Instuli from Industrie De Nora S.p.A. for assistance with XRD measurements.

The research was supported by Fondazione De Nora within a Fondazione Oronzio e Niccolò De Nora Fellowship in Applied Electrochemistry and by Università degli Studi di Milano by the “Piano di Sostegno alla Ricerca 2015-17”. Spectroscopic and EIS studies have been performed using instrumentation purchased through the National Science Centre, Poland - SONATA project UMO-2016/21/D/ST4/00221.

Appendix A. Supplementary data

Supplementary material related to this article can be found, in the online version, at doi:https://doi.org/10.1016/j.apcatb.2018.11.044.

References

[1] R. Daghrir, P. Drogui, D. Robert, Modified TiO_2 for environmental photocatalytic applications: a review, Ind. Eng. Chem. Res. 52 (2013) 3581–3599, https://doi.org/

10.1021/ie303468t.
[2] R. Beranek, J.M. Macak, M. Gärtner, K. Meyer, P. Schmuki, Enhanced visible light photocurrent generation at surface-modified TiO_2 nanotubes, Electrochim. Acta 54 (2009) 2640–2646, https://doi.org/10.1016/j.electacta.2008.10.063.
[3] M. Buchalska, J. Kuncewicz, E. Świętek, P. Łabuz, T. Baran, G. Stochel, W. Macyk, Photoinduced hole injection in semiconductor-coordination compound systems, Coord. Chem. Rev. 257 (2013) 767–775, https://doi.org/10.1016/j.ccr.2012.09.017.
[4] M. Aresta, A. Dibenedetto, T. Baran, S. Wojtyła, W. Macyk, Solar energy utilization in the direct photocarboxylation of 2,3-dihydrofuran using CO_2, Faraday Discuss. 183 (2015) 413–427, https://doi.org/10.1039/C5FD00040H.
[5] H. Park, Y. Park, W. Kim, W. Choi, Surface modification of TiO_2 photocatalyst for environmental applications, J. Photochem. Photobiol. C Photochem. Rev. 15 (2013) 1–20, https://doi.org/10.1016/j.jphotochemrev.2012.10.001.
[6] A. Gołąbiewska, M.P. Kobylański, A. Zaleska-Medynska, 2 - Fundamentals of Metal Oxide-based Photocatalysis, Met. Oxide-Based Photocatal., Elsevier, 2018, pp. 3–50, https://doi.org/10.1016/B978-0-12-811634-0.00002-0.
[7] R. Rodríguez, M.A. Blesa, A.E. Regazzoni, Surface Complexation at the TiO_2(anatase)/Aqueous Solution Interface: Chemisorption of Catechol, J. Colloid Interface Sci. 177 (1996) 122–131, https://doi.org/10.1006/jcis.1996.0012.
[8] F. De Angelis, A. Tilocca, A. Selloni, Time-dependent DFT Study of [Fe(CN)6]4-sensitization of TiO2 nanoparticles, J. Am. Chem. Soc. 126 (2004) 15024–15025, https://doi.org/10.1021/ja045152z.
[9] T. Sakata, K. Hashimoto, M. Hiramoto, New aspects of electron transfer on semiconductor surface: dye-sensitization system, J. Phys. Chem. 94 (1990) 3040–3045, https://doi.org/10.1021/j100370a056.
[10] T. Baran, W. Macyk, Photocatalytic oxidation of volatile pollutants of air driven by visible light, J. Photochem. Photobiol. Chem. 241 (2012) 8–12, https://doi.org/10.1016/j.jphotochem.2012.05.008.
[11] M. Aresta, A. Dibenedetto, T. Baran, A. Angelini, P. Labuz, W. Macyk, An integrated photocatalytic/enzymatic system for the reduction of CO_2 to methanol in bioglycerol-water, Beilstein J. Org. Chem. 10 (2014) 2556–2565, https://doi.org/10.3762/bjoc.10.267.
[12] S. Wojtyła, T. Baran, Photosensitization and photocurrent switching effects in wide band gap semiconductors: CuI and TiO_2 functionalized with iron and nickel complexes: from semiconductors to logic devices, J. Inorg. Organomet. Polym. Mater. 27 (2017) 436–445, https://doi.org/10.1007/s10904-016-0484-6.
[13] E. Galoppini, Light harvesting: strike while the iron is cold, Nat. Chem. 7 (2015) 861–862, https://doi.org/10.1038/nchem.2373.
[14] A. Morandeira, I. López-Duarte, M.V. Martínez-Díaz, B. O'Regan, C. Shuttle, N.A. Haji-Zainulabidin, T. Torres, E. Palomares, J.R. Durrant, Slow electron injection on Ru−phthalocyanine sensitized TiO_2, J. Am. Chem. Soc. 129 (2007) 9250–9251, https://doi.org/10.1021/ja0722980.
[15] L.F.O. Furtado, A.D.P. Alexiou, L. Gonçalves, H.E. Toma, K. Araki, TiO_2-based light-driven XOR/INH logic gates, Angew. Chem. Int. Ed. 45 (2006) 3143–3146, https://doi.org/10.1002/anie.200600076.
[16] S. Sumikura, S. Mori, S. Shimizu, H. Usami, E. Suzuki, Photoelectrochemical characteristics of cells with dyed and undyed nanoporous p-type semiconductor CuO electrodes, J. Photochem. Photobiol. Chem. 194 (2008) 143–147, https://doi.org/10.1016/j.jphotochem.2007.07.035.
[17] M.A. Barakat, J.M. Tseng, C.P. Huang, Hydrogen peroxide-assisted photocatalytic oxidation of phenolic compounds, Appl. Catal. B Environ. 59 (2005) 99–104, https://doi.org/10.1016/j.apcatb.2005.01.004.
[18] T. Baran, S. Wojtyła, A. Vertova, A. Minguzzi, S. Rondinini, Photoelectrochemical and photocatalytic systems based on titanates for hydrogen peroxide formation, J. Electroanal. Chem. Lausanne (Lausanne) 808 (2018) 395–402, https://doi.org/10.1016/j.jelechem.2017.06.044.
[19] Y. Shiraishi, S. Kanazawa, Y. Kofuji, H. Sakamoto, S. Ichikawa, S. Tanaka, T. Hirai, Sunlight-driven hydrogen peroxide production from water and molecular oxygen by metal-free photocatalysts, Angew. Chem. Int. Ed. 53 (2014) 13454–13459, https://doi.org/10.1002/anie.201407938.
[20] G. Satyabrat, K. Niranjan, Solar-driven hydrogen peroxide production using polymer-supported carbon dots as heterogeneous catalyst, Nano-Micro Lett. 9 (2017) 40.
[21] S. Zhao, X. Zhao, H. Zhang, J. Li, Y. Zhu, Covalent combination of polyoxometalate and graphitic carbon nitride for light-driven hydrogen peroxide production, Nano Energy 35 (2017) 405–414, https://doi.org/10.1016/j.nanoen.2017.04.017.
[22] Z. Wei, M. Liu, Z. Zhang, W. Yao, H. Tan, Y. Zhu, Efficient visible-light-driven selective oxygen reduction to hydrogen peroxide by oxygen-enriched graphitic carbon nitride polymers, Energy Environ. Sci. 11 (2018) 2581–2589, https://doi.org/10.1039/C8EE01316K.
[23] H. Eskandarloo, M.J. Selig, A. Abbaspourrad, In situ H_2O_2 generation for de-emulsification of fine stable bilge water emulsions, Chem. Eng. J. 335 (2018) 434–442, https://doi.org/10.1016/j.cej.2017.10.174.
[24] L. Abu-Ghunmi, M. Badawi, M. Fayyad, Fate of Triton x-100 applications on water and soil environments: a review, J. Surfactants Deterg. 17 (2014) 833–838, https://doi.org/10.1007/s11743-014-1584-3.
[25] Y. Zhang, Y. Wan, Heterogeneous photocatalytic degradation of Triton X-100 in aqueous TiO2 suspensions, Am. J. Environ. Prot. 3 (2014) 28, https://doi.org/10.11648/j.ajep.20140301.14.
[26] P. Hegedűs, E. Szabó-Bárdos, O. Horváth, K. Horváth, P. Hajós, TiO2-mediated photocatalytic mineralization of a non-ionic detergent: comparison and combination with other advanced oxidation procedures, Materials. 8 (2015) 231–250, https://doi.org/10.3390/ma8010231.
[27] S. Wojtyła, T. Baran, Insight on doped ZnS and its activity towards photocatalytic removing of Cr(VI) from wastewater in the presence of organic pollutants, Mater. Chem. Phys. 212 (2018) 103–112, https://doi.org/10.1016/j.matchemphys.2018.03.034.
[28] B. Czech, W. Ćwikła-Bundyra, Advanced oxidation processes in Triton X-100 and wash-up liquid removal from wastewater using modified TiO2/Al2O3 photocatalysts, Water Air Soil Pollut. 223 (2012) 4813–4822, https://doi.org/10.1007/s11270-012-1237-y.
[29] G. Pardo, R. Vargas, O. Núñez, Photocatalytic TiO_2 – assisted decomposition of Triton X-100: inhibition of p-nitrophenol degradation, J. Phys. Org. Chem. 21 (2008) 1072–1078, https://doi.org/10.1002/poc.1432.
[30] J. Saien, Z. Ojaghloo, A.R. Soleymani, M.H. Rasoulifard, Homogeneous and heterogeneous AOPs for rapid degradation of Triton X-100 in aqueous media via UV light, nano titania hydrogen peroxide and potassium persulfate, Chem. Eng. J. 167 (2011) 172–182, https://doi.org/10.1016/j.cej.2010.12.017.
[31] A. Di Paola, E. García-López, G. Marcì, L. Palmisano, A survey of photocatalytic materials for environmental remediation, J. Hazard. Mater. 211–212 (2012) 3–29, https://doi.org/10.1016/j.jhazmat.2011.11.050.
[32] H. Park, H. Kim, G. Moon, W. Choi, Photoinduced charge transfer processes in solar photocatalysis based on modified TiO2, Energy Environ. Sci. 9 (2016) 411–433, https://doi.org/10.1039/C5EE02575C.
[33] G. Moon, W. Kim, A.D. Bokare, N. Sung, W. Choi, Solar production of H2O2 on reduced graphene oxide–TiO_2 hybrid photocatalysts consisting of earth-abundant elements only, Energy Environ. Sci. 7 (2014) 4023–4028, https://doi.org/10.1039/C4EE02757D.
[34] M. Teranishi, S. Naya, H. Tada, In situ liquid phase synthesis of hydrogen peroxide from molecular oxygen using gold nanoparticle-loaded Titanium(IV) dioxide photocatalyst, J. Am. Chem. Soc. 132 (2010) 7850–7851, https://doi.org/10.1021/ja102651g.
[35] D. Tsukamoto, A. Shiro, Y. Shiraishi, Y. Sugano, S. Ichikawa, S. Tanaka, T. Hirai, Photocatalytic H_2O_2 production from Ethanol/O2 system using TiO_2 loaded with Au–Ag bimetallic alloy nanoparticles, ACS Catal. 2 (2012) 599–603, https://doi.org/10.1021/cs2006873.
[36] K. Xiong, K. Wang, L. Chen, X. Wang, Q. Fan, J. Courtois, Y. Liu, X. Tuo, M. Yan, Heterostructured ZnFe2O4/Fe2TiO5/TiO2 composite nanotube arrays with an improved photocatalysis degradation efficiency under simulated sunlight irradiation, Nano-Micro Lett. 10 (2017) 17, https://doi.org/10.1007/s40820-017-0169-x.
[37] R. Giovannetti, Ca.D. Amato, M. Zannotti, E. Rommozzi, R. Gunnella, M. Minicucci, A.D. Cicco, Visible light photoactivity of polypropylene coated Nano-TiO_2 for dyes degradation in water, Sci. Rep. 5 (2015), https://doi.org/10.1038/srep17801 srep17801.
[38] Bedri Erdem, Robert A. Hunsicker, Gary W. Simmons, E. David Sudol, Victoria L. Dimonie, M.S. El-Aasser, XPS and FTIR Surface Characterization of TiO_2 Particles Used in Polymer Encapsulation, (2001), https://doi.org/10.1021/la0015213.
[39] V.A. Zeitler, C.A. Brown, The infrared spectra of some Ti-O-Si, Ti-O-Ti and Si-O-Si compounds, J. Phys. Chem. 61 (1957) 1174–1177, https://doi.org/10.1021/j150555a010.
[40] A.G. Blackman, Encycl. inorg. bioinorg. Chem, Cobalt: Inorganic & Coordination Chemistry Based in Part on the Article Cobalt: Inorganic & Coordination Chemistry by David A. Buckingham Which Appeared in the Encyclopedia of Inorganic Chemistry, first edition, American Cancer Society, 2011, https://doi.org/10.1002/9781119951438.eibc0044.
[41] M. Subramanian, S. Vijayalakshmi, S. Venkataraj, R. Jayavel, Effect of cobalt doping on the structural and optical properties of TiO_2 films prepared by sol–gel process, Thin Solid Films 516 (2008) 3776–3782, https://doi.org/10.1016/j.tsf.2007.06.125.
[42] B.D. Viezbicke, S. Patel, B.E. Davis, D.P. Birnie, Evaluation of the Tauc method for optical absorption edge determination: ZnO thin films as a model system, Phys. Status Solidi B 252 (2015) 1700–1710, https://doi.org/10.1002/pssb.201552007.
[43] T.-L. Li, H. Teng, Solution synthesis of high-quality $CuInS_2$ quantum dots as sensitizers for TiO_2 photoelectrodes, J. Mater. Chem. 20 (2010) 3656–3664, https://doi.org/10.1039/B927279H.
[44] K. Rajeshwar, Fundamentals of Semiconductor Electrochemistry and Photoelectrochemistry, Encycl. Electrochem., Wiley-VCH, 2007, https://doi.org/10.1002/9783527610426.bard060001.
[45] M. Antuch, P. Millet, A. Iwase, A. Kudo, The role of surface states during photocurrent switching: Intensity modulated photocurrent spectroscopy analysis of $BiVO_4$ photoelectrodes, Appl. Catal. B Environ. 237 (2018) 401–408, https://doi.org/10.1016/j.apcatb.2018.05.011.
[46] W. Macyk, K. Szaciłowski, G. Stochel, M. Buchalska, J. Kuncewicz, P. Łabuz, Titanium(IV) complexes as direct TiO_2 photosensitizers, Coord. Chem. Rev. 254 (2010) 2687–2701, https://doi.org/10.1016/j.ccr.2009.12.037.
[47] Y. Nosaka, A.Y. Nosaka, Generation and detection of reactive oxygen species in photocatalysis, Chem. Rev. 117 (2017) 11302–11336, https://doi.org/10.1021/acs.chemrev.7b00161.
[48] D. Vasudevan, H. Wendt, Electroreduction of oxygen in aprotic media, J. Electroanal. Chem. Lausanne (Lausanne) 392 (1995) 69–74, https://doi.org/10.1016/0022-0728(95)04044-O.
[49] J.T. Adeleke, T. Theivasanthi, M. Thiruppathi, M. Swaminathan, T. Akomolafe, A.B. Alabi, Photocatalytic degradation of methylene blue by ZnO/$NiFe_2O_4$ nanoparticles, Appl. Surf. Sci. 455 (2018) 195–200, https://doi.org/10.1016/j.apsusc.2018.05.184.
[50] V. Vaiano, M. Matarangolo, J.J. Murcia, H. Rojas, J.A. Navío, M.C. Hidalgo, Enhanced photocatalytic removal of phenol from aqueous solutions using ZnO modified with Ag, Appl. Catal. B Environ. 225 (2018) 197–206, https://doi.org/10.1016/j.apcatb.2017.11.075.
[51] J. Zheng, H. Yu, X. Li, S. Zhang, Enhanced photocatalytic activity of TiO_2 nanostructured thin film with a silver hierarchical configuration, Appl. Surf. Sci. 254

(2008) 1630–1635, https://doi.org/10.1016/j.apsusc.2007.07.165.
[52] B. Xin, Z. Ren, P. Wang, J. Liu, L. Jing, H. Fu, Study on the mechanisms of photoinduced carriers separation and recombination for Fe^{3+}–TiO_2 photocatalysts, Appl. Surf. Sci. 253 (2007) 4390–4395, https://doi.org/10.1016/j.apsusc.2006.09.049.
[53] L. Wang, M. Bledowski, A. Ramakrishnan, D. König, A. Ludwig, R. Beranek, Dynamics of photogenerated holes in TiO2-polyheptazine hybrid photoanodes for visible light-driven water splitting, J. Electrochem. Soc. 159 (2012) H616–H622, https://doi.org/10.1149/2.010207jes.
[54] S. Wojtyła, W. Macyk, T. Baran, Photosensitization of CuI – the role of visible light induced $Cu^{I} \rightarrow Cu^{II}$ transition in photocatalytic degradation of organic pollutants and inactivation of microorganisms, Photochem. Photobiol. Sci. 16 (2017) 1079–1087, https://doi.org/10.1039/C6PP00465B.
[55] T. Fotiou, T.M. Triantis, T. Kaloudis, K.E. O'Shea, D.D. Dionysiou, A. Hiskia, Assessment of the roles of reactive oxygen species in the UV and visible light photocatalytic degradation of cyanotoxins and water taste and odor compounds using C–TiO_2, Water Res. 90 (2016) 52–61, https://doi.org/10.1016/j.watres.2015.12.006.
[56] S. Ledakowicz, D. Olejnik, J. Perkowski, H. Zegota, The use of advanced oxidation processes (AOP) for the decomposition of Triton X-114 nonionic detergent, Przemysl Chem. 80 (2001) 453–459.